Detection of Molecular Alignment in Confined Films

F. Eisert, M. Gurka, A. Legant, M. Buck,* M. Grunze

Optical second harmonic generation was used to study the in-plane alignment of self-assembled silane monolayers attached to a glass surface under mechanical loading. The measurements allow correlation of the macroscopic forces acting on the monolayer with the average orientation and the azimuthal molecular alignment of the terminal molecular entity. Compression and shear forces lead to an alignment of the initially randomly oriented molecules on a macroscopic length scale. The change in azimuthal alignment of molecules under mechanical stress was found to be irreversible on the time scale of 12 hours, whereas changes of the molecular tilt angle were reversible.

Tribological phenomena on molecular length scales are determined by the properties of the surfaces in contact. Sliding and friction are not only related to the topography and morphology of the interfaces but also to chemical surface composition. Among different concepts to chemically modify surfaces, monomolecular films are particularly attractive for tailoring surface properties. They are not only good models to study tribological phenomena but are actually used in microelectromechanical systems or disk drives (*1–3*). Despite numerous experimental (*1, 4–10*) and theoretical (*11–15*) studies, essential aspects of the mechanical properties of these layers are still not understood, for example, the time-dependent elastic response of an alkanethiolate monolayer. Some theoretical work (*11*) supported the experimental interpretation of force-induced entanglement and disorder (*4*), whereas other authors suggested a different explanation based on a structural rearrangement that retains efficient packing between the chains (*12*).

Obviously, it is important to observe the structure and molecular orientation in monolayer films in situ to fully understand the molecular changes in the confined space between the two surfaces, because these may be reversible. A combination of force and structure measurements has been reported for thick liquid crystal films using x-ray scattering in the gap of a surface force apparatus (*16*), and infrared spectroscopy has been combined with a sliding device to study elastohydrodynamic contacts (*17, 18*). However, for monolayers confined between two surfaces, linear optical techniques are not sensitive enough, and, so far, only nonlinear optical spectroscopies have been successfully applied (*5, 6*).

Here, we used second harmonic generation (SHG) as an interface-sensitive and noninvasive technique to investigate the behavior of a molecular monolayer under confinement (*19, 20*). Although similar to the experiments reported before (*5, 6*), we implemented two decisive differences: First, a different detection scheme was used that allowed us to infer the in-plane symmetry of the film, and, second, the mechanical design was such that shear forces along defined directions could be applied to the film (Fig. 1).

A monolayer of *N*-[3-(trimethoxysilyl) propyl 2,4-dinitrophenylamine] [$(NO_2)_2$-C_6H_3-NH-$(CH_2)_3$-$Si(OCH_3)_3$ (DNS)] adsorbed on an SF10 glass prism (*21*) (index 1) was loaded by pressing a plano-convex BK7 glass lens (index 2) against it. Irradiating the layer with a pulsed laser (30 ps at 1064 nm) generates a second harmonic signal at 532 nm from the aromatic moiety, whose nonlinear optical properties have been characterized in detail (*22*). Recording the SHG signal at fixed polarization as a function of the input polarization yields information about the in-plane orientation (with respect to the underlying surface) and the tilt angle of the 2,4-dinitroaniline groups. By focusing the laser beam to a diameter of about 100 μm, a lateral map of the SHG signal of the contact area between lens and prism could be recorded.

In the first type of experiment (Fig. 1A), the lens was pressed against the prism with its center line parallel to the surface normal. Applying a load of $F = 40$ N produces a circular contact area of about 1.2 mm in diameter, as estimated from the spatial map. This agrees very well with the value of 1.16 mm calculated from Hertz's theory of elastic contacts (*23, 24*). A mean contact pressure of $P_m \approx 37$ MPa results. The pressure is large enough to flatten the surfaces of the two solids by elastic deformation (*5*). Because of the symmetry of the experiment, shear forces are radially symmetric.

In the second type of experiment, the lens was rolled over the prism (Fig. 1B). The same load was applied. For this experiment, shear forces occur preferentially along the rolling direction. The reaction of the organic layer to normal and shear forces is monitored by record-

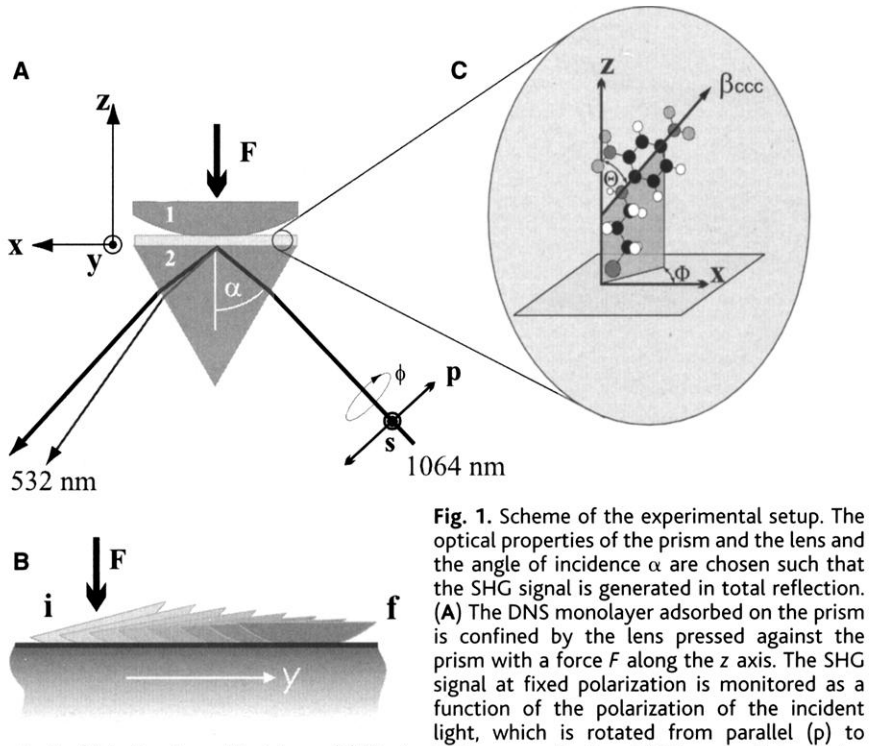

Fig. 1. Scheme of the experimental setup. The optical properties of the prism and the lens and the angle of incidence α are chosen such that the SHG signal is generated in total reflection. (**A**) The DNS monolayer adsorbed on the prism is confined by the lens pressed against the prism with a force *F* along the z axis. The SHG signal at fixed polarization is monitored as a function of the polarization of the incident light, which is rotated from parallel (p) to perpendicular (s) to the plane of incidence. (**B**) Mechanical forces applied to a DNS layer by first pressing the lens in a canted orientation against the prism at point *i* and then rolling over the prism surface in a defined direction to the final position *f*. (**C**) Illustration of an adsorbed DNS molecule. As indicated by the arrow, SHG monitors the dinitroaniline moiety and thus allows inference of its tilt angle Θ and its in-plane symmetry determined by the distribution function of the azimuthal angle Φ.

Lehrstuhl für Angewandte Physikalische Chemie, Im Neuenheimer Feld 253, 69120 Heidelberg, Germany.

*To whom correspondence should be addressed. E-mail: cv6@ix.urz.uni-heidelberg.de

ing the intensity of the second harmonic signal (*19, 20, 25*):

$$I_i^{2\omega} \propto \left| E_0^{(\omega)} E_0^{(\omega)} \sum_{jk} L_{ijk}\chi_{ijk}(\beta,\Theta,\Phi) f_j(\phi) g_k(\phi) \right|^2 \qquad i,j,k\ldots x,y,z \qquad (1)$$

The indices i,j,k refer to the axes of the Cartesian coordinate system defined in Fig. 1. The amplitude of the electric field of the incident wave is described by $E_0^{(\omega)}$, and the effective field in the organic layer is taken into account by the Fresnel factors L_{ijk}. $f_j(\phi)$ and $g_k(\phi)$ define the projections of the electric field vector of the incident beam onto the respective coordinate axes. ϕ defines the angle of polarization with respect to the plane of incidence. In our experiments, where ϕ is continuously varied between 0° and 360°, f_j and g_k are either cosine or sine functions. The molecular information is contained in the susceptibility χ, which is a third rank tensor. The number of nonvanishing independent elements is determined by the nature of the second harmonic active molecular moiety and the in-plane symmetry of the film, which are represented by the hyperpolarizability tensor β and the distribution function of the azimuthal orientation Φ of the molecules, respectively. If the nonlinear optical properties of the molecules are known, for example, determined by β_{ccc} (Fig. 1C), their average tilt angle Θ can be determined. The second harmonic signal polarized along a direction i is determined by a superposition of different susceptibility elements (Eq. 1) (*26*). The number of contributing tensor elements determines the ϕ dependence of the second harmonic signal.

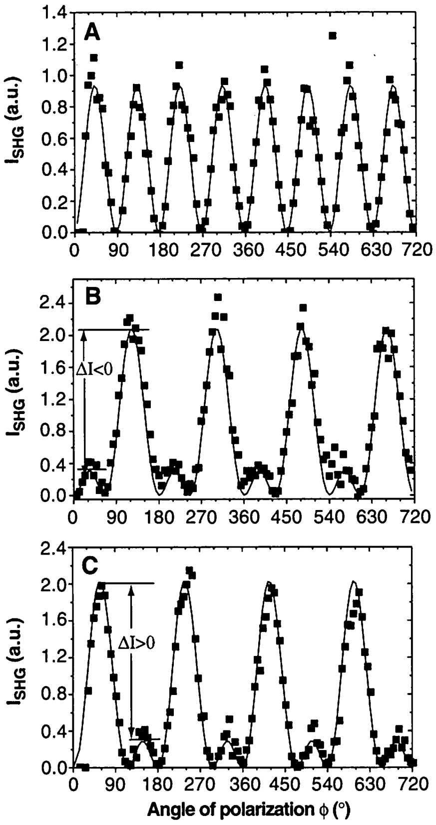

Fig. 2. s-polarized SHG signal (squares) as a function of the angle ϕ of the input polarization and fits (solid line) based on Eq. 1. For better statistics, two full rotations of the polarization are measured. (**A**) Unloaded monolayer. (**B** and **C**) Confined monolayer. The lens was rolled in $+y$ (B) and $-y$ (C) directions (for details, see text).

As the number of nonvanishing tensor elements depends on the in-plane symmetry of the interface, that is, the distribution function of the azimuthal angle Φ, SHG can probe force-induced changes of the symmetry of the molecular layer. In the most simple case, where the second harmonic signal is polarized parallel to the substrate (s polarization), only one tensor element contributes in the case of an azimuthal symmetry ($C_{\infty v}$). As a result, the SHG signal exhibits a periodic variation as a function of ϕ with all maxima being of equal height (Fig. 2A), indicating a random distribution of the molecular entities with respect to Φ, as expected for a pristine, unloaded monolayer. In contrast, in the case of mirror symmetry (C_s), four tensor elements interfere. This yields a more complex shape of the SHG signal with maxima of different height, which, in addition, can differ in their sequence (Fig. 2, B and C). The microscopic interpretation of alternating maxima is that molecules adopt a preferential orientation along an axis in the x-y plane. The sequence reveals whether the alignment is parallel or antiparallel to this axis. Taking the difference ΔI between adjacent maxima as a convenient measure for the in-plane anisotropy and the direction of alignment of molecular entities, rolling along the $+y$ direction produces alternating maxima with $\Delta I < 0$ (Fig. 2B).

The alignment can be inverted by rolling into the opposite ($-y$) direction (Fig. 2C). ΔI is now positive and indicates that the second harmonic active moiety is now pointing into the opposite direction. Within the time periods of our experiments (up to 12 hours), the alignment of the molecules induced by rolling the lens persists after the film is unloaded. Without going into details, we note that upon loading, the polar orientation as expressed by the tilt angle Θ (Fig. 1C) of the dinitroaniline moieties also changes. However, in contrast to the azimuthal alignment, this change of the tilt angle is reversible. It returns instantaneously to the unloaded value within the time resolution of our experiment, which is on the order of seconds (*27*).

Laterally resolved measurements of ΔI reveal a pronounced dependence of the alignment on the applied stress. Three different situations were realized: loading along the surface normal (Fig. 3A) and loading and rolling in the $+y$

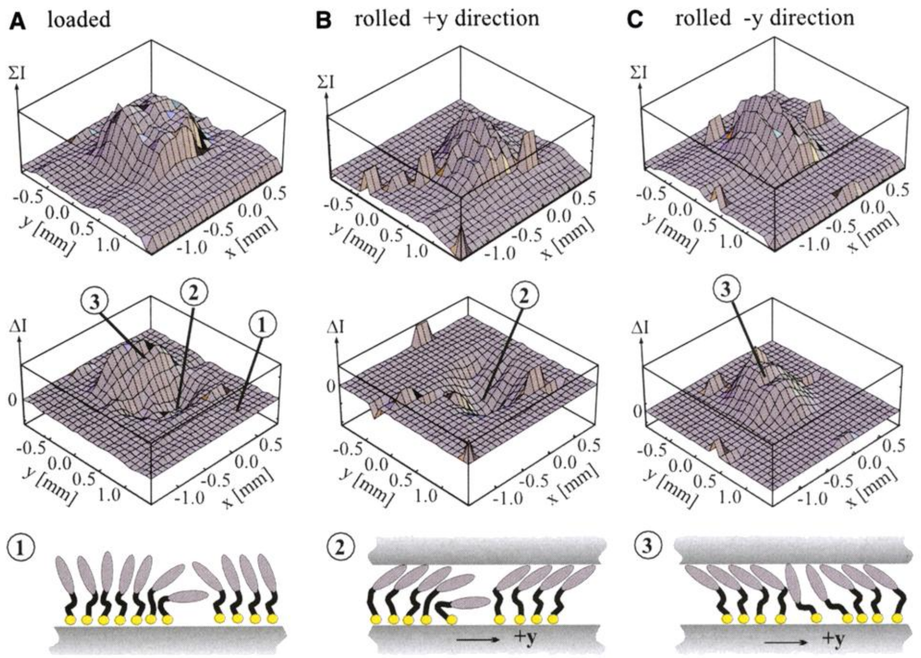

Fig. 3. Laterally resolved scans of a DNA layer. s-polarized SHG signal recorded for a film under normal load (**A**) and under shearing along the $+y$ (**B**) and $-y$ (**C**) directions. The topmost intensity maps represent the sum ΣI of the maxima around ϕ = 45° and ϕ = 135° (see Fig. 2). The middle panels depict maps of the difference ΔI, which is a measure of the alignment of the dinitroaniline moieties. In (A), ΔI changes sign along the y direction within the contact area. The sign change occurs at the point of initial contact defined by the origin of the coordinate system between the lens and the prism and is due to the radial alignment of the molecules. In (B) and (C), ΔI is either larger or smaller than zero. This indicates a unidirectional alignment within the contact area that is controlled by the direction of the shear force. The lower panels provide an illustration of the structure of the film at selected points that represent the film not loaded (1) and rolled in $+y$ (2) and $-y$ (3) directions.

(Fig. 3B) and $-y$ (Fig. 3C) directions. All three experiments were performed with pristine films. The upper panels show the sum ΣI of two adjacent intensity maxima as shown in Fig. 2. The angle of incidence of the fundamental beam was chosen such that the Fresnel factors are higher at the lens-prism interface compared with the prism-air interface (*6*). Thus, the area of increased SHG intensity directly reflects the size of the contact area. The middle panels show maps of ΔI. For normal loading of the lens (Fig. 3A), ΔI changes sign across the contact area, indicating that the forces are axially symmetric with respect to the initial point of contact, causing a radial alignment of the molecules. Because we only probed alignment along the y axis, $|\Delta I|$ for molecules aligned along the x axis is zero and gradually increases with increasing alignment along y. This is seen in the radially symmetric case in which ΔI changes sign at $y = 0$. In contrast, rolling causes a unidirectional alignment over the whole contact area (Fig. 3, B and C).

It is evident from the alignment seen under both normal loading and rolling conditions that shear forces act on the film. However, their origin is not clear at present. Microslip due to the difference in the elastic constants of the prism and the lens seems to be too small to account for the alignment, and, furthermore, an alignment pattern different from those depicted in Fig. 3, B and C, is expected from standard models in contact mechanics (*23*). Thus, other mechanisms should be considered, such as squeezing of the organic film, which would produce a lateral force originating from the point of highest pressure outward. Also, interfacial contaminations such as an adsorbed water film that is squeezed out of the contact area under loading could give rise to an additional shear force.

The results presented here demonstrate that the tribological properties of surface coatings and lubricants between two bodies can be monitored in situ to study molecular changes as a function of loading conditions and to monitor their durability or wear. They can be extended to sum frequency generation (SFG) (*28*) studies, which will then allow the study of confined organic films more relevant to technical applications than the model system presented here.

References and Notes

1. B. Bhushan, J. N. Israelachvili, U. Landman, *Nature* **374**, 607 (1995).
2. R. Maboudian, *MRS Bull.* (June 1998), p. 47.
3. J. A. Harrison and S. S. Perry, *MRS Bull.* (June 1998), p. 27.
4. S. A. Joyce, R. C. Thomas, J. E. Houston, T. A. Michalske, R. M. Crooks, *Phys. Rev. Lett.* **68**, 2790 (1992).
5. Q. Du *et al.*, *Phys. Rev. B* **51**, 7456 (1995).
6. R. Frankel, G. E. Butterworth, C. D. Bain, *J. Am. Chem. Soc.* **120**, 203 (1998).
7. A. Berman, S. Steinberg, S. Campbell, A. Ulman, J. Israelachvili, *Tribol. Lett.* **4**, 43 (1998).
8. J. N. Israelachvili and D. Tabor, *Nature* **241**, 148 (1973).
9. J. N. Israelachvili, *J. Vac. Sci. Technol. A* **10**, 2961 (1992).
10. G. Liu and M. Salmeron, *Langmuir* **10**, 367 (1994).
11. S. Karaborni, *Phys. Rev. Lett.* **73**, 1668 (1994).
12. K. J. Tupper and D. Brenner, *Langmuir* **10**, 2335 (1994).
13. K. J. Tupper, R. J. Colton, D. W. Brenner, *Langmuir* **10**, 2041 (1994).
14. R. Henda, M. Grunze, A. J. Pertsin, *Tribol. Lett.* **5**, 191 (1998).
15. J. I. Siepmann and I. R. McDonald, *Langmuir* **9**, 2351 (1993).
16. S. H. J. Idziak *et al.*, *Science* **264**, 1915 (1994).
17. P. M. Cann and H. A. Spikes, *Tribol. Trans.* **34**, 248 (1991).
18. G. J. Johnston, R. Wayte, H. A. Spikes, *Tribol. Trans.* **34**, 187 (1991).
19. Y. R. Shen, *The Principles of Nonlinear Optics* (Wiley, New York, 1984).
20. R. M. Corn and D. A. Higgins, *Chem. Rev.* **94**, 107 (1994).
21. The sample preparation followed (29) with the use of a solution of *N*-[3-(trimethoxysilyl)propyl 2,4-dinitrophenylamine] in toluene.
22. D. S. Chemla and J. Zyss, Eds., *Nonlinear Optical Properties of Organic Molecules and Crystals*, vol. 1 (Academic Press, Orlando, FL, 1987).
23. K. L. Johnson, *Contact Mechanics* (Cambridge Univ. Press, Cambridge, 1985).
24. The following data were used in the calculation. The radius of the curvature of the lens was 250 mm. Elastic moduli of the SF10 glass prism and the BK7 glass lens were 64 GN/m^2 and 82 GN/m^2, respectively. The Poisson ratios were 0.23 for SF10 and 0.206 for BK7.
25. B. U. Felderhof, A. Bratz, G. Marovsky, O. Roders, F. Sieverdes, *J. Opt. Soc. Am. B* **10**, 1824 (1993).
26. Because a detailed treatment is beyond the scope of this report, we make the simplifying assumption that the signal originates only from the organic layer. This does not hold exactly (*27*) but can be neglected for the purpose of this report.
27. A. Legant, thesis, University of Heidelberg, Heidelberg, Germany (1999).
28. C. D. Bain, in *Modern Characterization Methods of Surfactant Systems*, B. P. Binks, Ed. (Dekker, New York, 1999), pp. 336–373.
29. K. Bierbaum *et al.*, *Langmuir* **11**, 512 (1995).
30. This work was funded by the Office of Naval Research. Additional support from the Deutsche Forschungsgemeinschaft and the Fond der Chemischen Industrie is gratefully acknowledged. We are grateful to W. Eck for purifying the DNS.

1 September 1999; accepted 22 November 1999

Ultrafast Mid-Infrared Response of $YBa_2Cu_3O_{7-\delta}$

R. A. Kaindl,[1] M. Woerner,[1] T. Elsaesser,[1]* D. C. Smith,[2] J. F. Ryan,[2] G. A. Farnan,[3] M. P. McCurry,[3] D. G. Walmsley[3]

Optical spectra of high-transition-temperature superconductors in the mid-infrared display a gap of in-plane conductivity whose role for superconductivity remains unresolved. Femtosecond measurements of the mid-infrared reflectivity of $YBa_2Cu_3O_{7-\delta}$ after nonequilibrium optical excitation are used to demonstrate the ultrafast fill-in of this gap and reveal two gap constituents: a picosecond recovery of the superconducting condensate in underdoped and optimally doped material and, in underdoped $YBa_2Cu_3O_{7-\delta}$, an additional subpicosecond component related to pseudogap correlations. The temperature-dependent amplitudes of both contributions correlate with the antiferromagnetic 41-millielectronvolt peak in neutron scattering, supporting the coupling between charges and spin excitations.

A number of energy-sensitive studies on high-transition-temperature (high T_C) cuprate superconductors including tunneling (*1*), angular-resolved photoemission (*2*), neutron scattering (*3*), Raman scattering (*4*), and infrared reflectivity (*5–8*) suggest that understanding the elementary excitations in the mid-infrared energy range ($\hbar\omega \approx 40$ to 200 meV) in the vicinity of the superconducting gap is essential for clarifying the mechanisms behind formation of the superconducting condensate. In particular, the low-energy electromagnetic response of such cuprates contains valuable information on electronic excitations and their correlated dynamics. When temperature T is lowered below the superconducting transition in optimally doped materials, the most pronounced changes of the reflectivity $R(\omega,T)$ for light of frequency ω polarized parallel to the superconducting CuO_2 planes [(ab)-plane reflectivity] appear in the spectral range around $\hbar\omega \approx 100$ meV. These reflectivity changes (Fig. 1A) are directly connected with a strong depression of the in-plane conductivity (Fig. 1C), which has been attributed to the opening of a gap for electronic transitions involving inelastic collisions. A straightforward association with the superconducting gap, however, is hampered by the observation that, in underdoped cuprates, such features already occur at temperatures T^* substantially higher than T_C (Fig. 1, B and D) and are termed pseudogap (*5–8*).

While stationary infrared spectroscopy measures the total of all contributions to the mid-infrared reflectivity and cannot clearly discern spectrally similar components in the pseudogap

---

[1] Max-Born-Institut für Nichtlineare Optik und Kurzzeitspektroskopie, D-12489 Berlin, Germany. [2] Department of Physics, Clarendon Laboratory, Oxford University, Oxford OX1 3PU, UK. [3] Department of Pure and Applied Physics, Queen's University of Belfast, Belfast BT7 1NN, UK.

*To whom correspondence should be addressed.